Analytical expressions of the dynamic magnetic power loss under alternating or rotating magnetic field

Benjamin Ducharne, G. Sebald

Analytical expressions of the dynamic magnetic power loss under alternating or rotating magnetic field

B. Ducharne[1,2,✉], G. Sebald[1]

[1] ELyTMaX IRL3757, CNRS, Univ. Lyon, INSA Lyon, Centrale Lyon, Université Claude Bernard Lyon 1, Tohoku University, Sendai, Japan.

[2] Univ Lyon, INSA-Lyon, LGEF EA682, F69621, France.

Abstract

Analytical methods are recommended for rapid predictions of the magnetic core loss as they require less computational resources and offer straightforward sensitivity analysis. This paper proposes analytical expressions of the dynamic magnetic power loss under an alternating or rotating magnetic field. The formulations rely on fractional derivative analytical expressions of trigonometric functions. The simulation method is validated on extensive experimental data obtained from state-of-the-art setups and gathered in the scientific literature. Five materials are tested for up to at least 1 kHz in both alternating and rotating conditions. The relative Euclidean distance between the simulated and experimentally measured power loss is lower than 5 % for most tested materials and always lower than 10%. In standard characterization conditions, i.e., sinusoidal flux density, the dynamic power loss contribution under a rotating magnetic field is shown to be precisely two times higher than an alternating one. The knowledge of electrical conductivity reduces the dynamic magnetic power loss contribution to a single parameter (the fractional order). This parameter has the same value for a given material's rotational and alternating contribution. This study confirms the viscoelastic behavior of the magnetization process in ferromagnetic materials and, consequently, the relevance of the fractional derivative operators for their simulation.

Keywords

Alternating magnetization, rotational magnetization, fractional derivative, viscoelastic behavior, core loss prediction.

I – Introduction

Predicting magnetic losses is crucial in designing and optimizing electromagnetic converters, such as transformers, inductors, and motors. Magnetic losses can significantly impact the efficiency, performance, and effectiveness of these devices. Magnetic losses contribute to energy dissipation in the form of heat; excessive heat can lead to temperature rise issues, affecting the reliability and lifespan of the converters [1]. Accurate predictions help estimate the temperature rise and implement appropriate cooling mechanisms to ensure the converter operates within acceptable temperature limits [2]. Magnetic losses influence the size and weight of electromagnetic devices, and forecasting them allows designers to strike a balance between efficiency and size, meeting specific application requirements.

Soft Ferromagnetic Materials (SFMs) exhibit various magnetic properties, and a good knowledge of the working conditions and losses drives the selection of the appropriate ones. Eventually, adequately selecting materials contributes to developing environmentally friendly technologies that consume less energy and reduce overall environmental impact.

While the choice of the working frequencies depends on the application, there are multiple reasons for higher frequencies to be preferred. At higher frequencies, the size of magnetic components is reduced, leading to compact and lightweight converters. Higher-frequency working conditions allow one for transferring more power within the same physical space. It is particularly advantageous in applications where space and weight are critical parameters (portable electronic devices, aerospace systems, etc.) [3-5].

Different techniques exist to model the magnetic losses in an electromagnetic converter [6, 7]. These methods form two categories: the analytical and the numerical techniques.
_ The analytical methods are helpful as they provide rapid estimation and require less computational resources. They can offer deeper insights into the physical mechanisms and straightforward sensitivity analysis. The analytical methods include the well-known Steinmetz Equation (Eq. 1), a widely used empirical formula that estimates the total core loss in magnetic materials.

$$P_v = k \cdot f^a \cdot {B_M}^b \quad (1)$$

Here, P_v is the time average power loss per unit volume, f is the frequency, and B_M is the peak magnetic flux density. k, a, and b, called the Steinmetz coefficients, are material parameters generally found empirically by curve fitting. Eq. 1 is straightforward; however, even if it provides a valuable approximation for calculating hysteresis losses in ferromagnetic materials under standard magnetic fields, more sophisticated models and experiments may be required for accurate predictions. This statement is especially valid in the high-frequency range promoted by contemporary applications and the quest for higher power density. The more recent Bertotti's Statistical Theory of Losses (STL [8,9]) provides a statistical framework for understanding and predicting losses in ferromagnetic materials. It describes how the losses in such materials due to

hysteresis, eddy currents, and excess effects are influenced by stochastic processes, offering a detailed approach for modeling these losses analytically.

_ The numerical techniques include space-discretized methods like the finite element (FE) or the Finite Difference (FD) analysis [10, 11]. These methods allow one for detailed modeling of complex geometries and material properties, enabling the prediction of magnetic losses with superior accuracy. While space-discretized techniques have proven to be powerful tools, they come with complexities. Those include the mesh generation, the element selection, the definition of the boundary conditions, etc. In the electromagnetic domain, coupling the Maxwell equations and the highly nonlinear behavior of ferromagnetic materials represents the most significant challenge [12]. Space-discretized methods are more advantageous than analytical methods in specific scenarios. However, their implementation is time-consuming, and convergence is unpredictable.

This work aims to provide a simple, still efficient solution for accurately predicting the magnetic loss on a wide frequency range under alternating or rotating magnetization processes. The space-discretized solutions were discarded for complexity, and we opted for an analytical solution. For accurate results in an extensive frequency range, we looked for mathematical operators balancing the dynamic behavior differently than Eq. 1. Such operators exist in the framework of fractional calculus [13]. International standards rule the characterization of magnetic materials. These standards impose the average flux density as sinusoidal for proper and comparable characterization [14-16]. This is a challenge to implement such kind of waveform in experiments as the relations between the magnetic quantities and the imposed electrical ones are highly nonlinear. Still, from the viewpoint of analytical predictions, it can be seen as good news as analytical expressions exist for fractional derivatives and integrals of trigonometric waveforms [17].

In this work, an analytical expression based on fractional derivative operators was proposed to predict the dynamical magnetic loss power of SFMs. After that, we gathered as much experimental data as possible from the scientific literature. We collected magnetic loss under alternating and rotating magnetization for an extensive range of classical SFMs and on large frequency bandwidths. Then, we ran an optimization process to obtain the simulation parameters. We observed that once the electrical conductivity was known, a single dynamical parameter was enough to predict the dynamical magnetic loss power for all the materials tested precisely. In recent papers, fractional derivative operators have already been proven suitable mathematical tools for predicting magnetic core loss. However, the analytical expression simplicity outlined in this new research and its extensive validation on a large scale, encompassing alternating and rotational magnetization conditions, represents noteworthy progress in comprehending the dynamic behavior of SFMs. This paper provides an overview of the simulation method, incorporating an introduction to fractional calculus and its applicability within the framework of SFMs. Numerical simulations and experimental measurements are compared for different materials and used to validate the theoretical approach. The last section gives discussions and is followed by a conclusion.

II – Simulation method

The historical development of simulation methods for magnetic power loss is closely tied to advancements in computational techniques, the understanding of magnetic materials, and the growing demand for more efficient electrical devices [6, 18]. Even if analytical methods have been used less than numerical ones recently, fractional derivative operators balancing the dynamical content differently than entire ones open new perspectives.

2.1 – Time-fractional derivative: physical meaning in a magnetic power loss context and resolution

Fractional calculus originated in the 17th century when mathematicians like Leibniz and de L'Hôpital proposed to generalize the concept of differentiation and integration to non-integer orders, leading to the development of fractional calculus as a distinct branch of mathematical analysis [19]. Fractional derivatives are non-local by definition. Where classical time derivatives can only describe variations in adherent time instants t, fractional ones consider the entire simulated time interval [20, 21]. Consequently, time fractional derivatives are suggested for scenarios with prolonged heavy tail decays encompassing the complete historical context. This property suits the magnetic behavior of SFMs, which are known to be notably history-dependent.

Different definitions of fractional derivatives exist. The choice of a specific definition often depends on the context of the mathematical, physical, and engineering problem being addressed. Trigonometric functions possess a unique property known as analyticity, which results from satisfying the Laplace equation and the Cauchy-Riemann equations [22]. This property allows for the use of fractional calculus techniques to describe the behavior of trigonometric functions under fractional differentiation, which, in other words, means that they possess analytical fractional derivative solutions:

$$\frac{d^n}{dt^n}\sin(\omega t) = \omega^n \sin\left(\omega t + n\frac{\pi}{2}\right) \tag{2}$$

First-order derivation in the calculus of magnetic power loss implies that all losses are dissipative; however, the magnetization process includes interactions between the magnetic domains and displacements of the magnetic wall separating them. These motions appear to be not only viscous but also elastic. Such viscoelastic behavior can be obtained using fractional derivative operators (Eq. 2, where *n* is the fractional order that sets the ratio between the viscous and the elastic contributions). A similar behavior can be observed in mechanics [23, 24]. In this domain, the predominant models describing viscoelastic response are called 'mechanistic' models, wherein combinations of springs and dashpots arranged in series and/or parallel configurations are used to simulate the material behavior [25]. Springs are associated with the response of elastic solids, where stress is directly proportional to strain, corresponding to a 0^{th}-order derivative term. Conversely, dashpots symbolize the response of viscous fluids, with stress being proportional to strain rate, representing a 1^{st}-order derivative term. The concept of employing a fractional derivative of order *n*, where $0 < n < 1$, to characterize a viscoelastic material is derived from the

premise that the actual response of such material lies between a 0th and 1st-order derivative, effectively bridging the characteristics of an elastic solid and a viscous fluid [25].

2.2 – Simulation method of the magnetic power loss

2.2.1 Alternating magnetization conditions

In alternating magnetization conditions (Fig. 1 – b), the magnetic power loss P_{alt} in SFMs can be separated into two contributions:

$$P_{alt} = P_{stat\ alt} + P_{dyn\ alt} \tag{3}$$

_ $P_{stat\ alt}$ is a quasi-static contribution independent of the working frequency. $P_{stat\ alt}$ can be estimated by calculating the hysteresis loop area $B_a(H_{surf})$, where B_a is the flux density averaged through the tested specimen cross-section and $H_{surf\ stat}$ is the tangent excitation field, measured in the very low-frequency range (f_{stat} = 1/T_{stat}). This contribution is usually called hysteresis loss (STL, [8]).

$$P_{stat\ alt} = \frac{1}{T_{stat}\delta}\int_0^{T_{stat}} \frac{dB_a}{dt} \cdot H_{surf\ stat} dt \tag{4}$$

Here, δ is the simulated material density.

_ P_{dyn} is a dynamic contribution (frequency-dependent). This contribution reflects the material's inability to follow rapid changes in magnetic excitation. Those include the difficulty for the magnetic domains to reorganize rapidly; this contribution is called excess loss in STL. The other contribution is called classical loss or eddy current loss. It is caused by circulating currents induced in the tested specimen due to variations in the excitation. According to the skin effect, the eddy current tends to flow more on the material's surface as the frequency increases, leading to increased resistance and higher losses. In STL, both contributions are calculated separately. Still, a single term is enough to provide correct simulation predictions in our proposed method.

For a given B_a, the dynamic tangent excitation field $H_{surf\ dyn}$ can be separated into $H_{surf\ stat,}$ and a dynamic term H_{dyn}, the product of ρ, a constant depending on the geometry and nature of the tested material (its unit is A·V^{-n}·m^{2n-1}), and the n time-fractional derivative of B_a (Eq. 5, 6) [26-28].

$$H_{surf\ dyn} = H_{surf\ stat} + H_{dyn} \tag{5}$$

$$H_{dyn} = \rho \cdot \frac{d^n B_a}{dt^n} \tag{6}$$

The dynamic power loss contribution P_{AC} is expressed as:

$$P_{dyn\ alt} = \frac{1}{T\delta} \cdot \int_0^T \frac{dB_a}{dt} \cdot H_{dyn} dt = \frac{1}{T\delta} \cdot \int_0^T \frac{dB_a}{dt} \cdot \rho \cdot \frac{d^n B_a}{dt^n} dt \tag{7}$$

The unique presence of B_a as a time-dependent quantity in Eq. 7 is worth noting. As B_a is described with a trigonometric function (imposed by the international standards for the SFMs characterization), an analytical expression of P_{dyn} can be derived.

$$B_a = B_M \sin(\omega t) \tag{8}$$

$$P_{dyn\ alt} = \frac{\rho}{2\delta} B_M \omega^{n+1} \sin\left(n\frac{\pi}{2}\right) \tag{9}$$

$$P_{alt} = \frac{1}{T_{stat}\delta}\int_0^{T_{stat}} \frac{dB_a}{dt} \cdot H_{surf\ DC} dt + \frac{\rho}{2\delta} B_M \omega^{n+1} \sin\left(n\frac{\pi}{2}\right) \quad (10)$$

2.2.2 Rotational magnetization conditions

Throughout a cycle of alternating excitation, the magnetic material experiences a sequence of positive and negative magnetic field strengths. Whatever H_{surf} amplitude, a $B_a(H_{surf})$ hysteresis loop is consistently formed, and with heightened excitation, the response amplifies. Notably, even at full saturation, there remains a potential for an increase in B_a, which, during dynamic magnetization, contributes to elevated eddy current loss. Consequently, the cumulative losses under alternating excitation consistently rise with the level of excitation [29](see Fig. 1 – (a)).

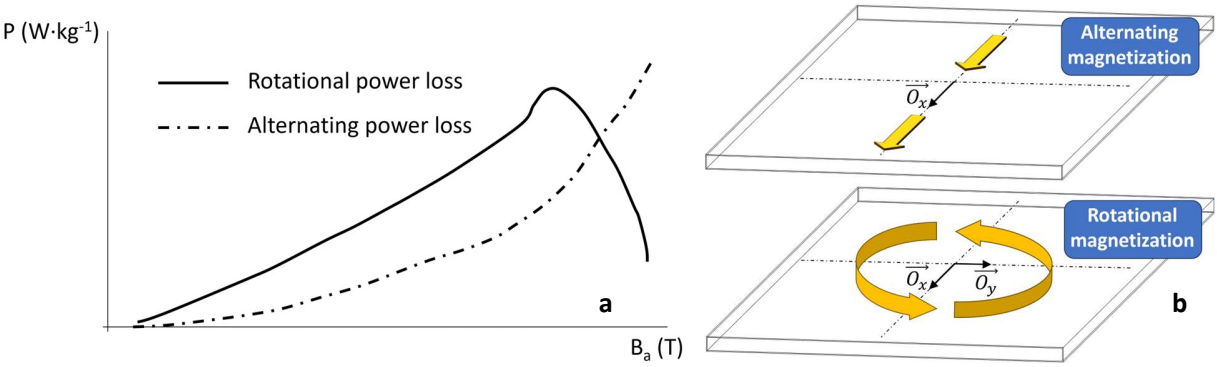

Fig. 1 – (a) Power loss characteristics for oriented grain electrical steel (GOFeSi) sheet under alternating and rotational magnetization [27]. (b) Alternating and rotational magnetization illustration.

The situation is very different under rotational magnetization. Under moderate H_{surf} amplitude, when the excitation rotates, the domain structure undergoes continuous and more intricate changes than under alternating conditions, leading to increased rotational losses. However, the rotational loss decreases sharply above a certain level of H_{surf} amplitude. This behavior occurs because the magnetic domains begin to merge at a sufficiently high excitation; hence, some domain walls are eliminated. Because hysteresis and excess loss components (in the STL context [8, 9]) are linked to domain wall movements, the two components are proportionally diminished, reducing the total loss significantly. In the higher dynamic range, eddy currents persist, leading to an increased effect of the magnetic loss. The total loss can theoretically diminish to zero at complete saturation in quasi-static circumstances.

The formula for the rotational losses in the so-called field metric technique is reminded below [30] (see Fig. 1 – (b)) :

$$P_{rot} = \frac{1}{T\delta} \cdot \int_0^T \left(\frac{dB_{ax}}{dt} \cdot H_{surfx} + \frac{dB_{ay}}{dt} \cdot H_{surfy}\right) dt \quad (11)$$

Here, B_{ax}, B_{ay}, H_{surfx}, and H_{surfy} are the projections of B_a and H_{surf} along the x and y-axes, respectively [31, 32]. Similarly to alternating magnetization, P_{rot} in rotational conditions can be separated into a quasi-static and a dynamic contribution:

$$P_{rot} = P_{stat\,rot} + P_{dyn\,rot} \tag{12}$$

_ P_{stat} becomes:

$$P_{stat\,rot} = \frac{1}{T_{stat}\delta}\int_0^{T_{stat}} \left(\frac{dB_{ax}}{dt}\cdot H_{surfx\,DC} + \frac{dB_{ay}}{dt}\cdot H_{surfy\,DC}\right) dt \tag{13}$$

_ Under rotational B_a conditions, both B_{ax} and B_{ay} exhibit trigonometric behaviors that are amendable to analytical solutions based on fractional derivatives:

$$\begin{cases} B_{ax} = B_M \sin(\omega t) \\ B_{ay} = B_M \cos(\omega t) \end{cases} \tag{14}$$

$$P_{dyn\,rot} = \frac{1}{T\delta}\cdot\int_0^T \left(\frac{dB_{ax}}{dt}\cdot H_{dynx} + \frac{dB_{ay}}{dt}\cdot H_{dyny}\right) dt = \frac{\rho}{T\delta}\int_0^T \left(\frac{dB_{ax}}{dt}\cdot\frac{d^nB_{ax}}{dt^n} + \frac{dB_{ay}}{dt}\cdot\frac{d^nB_{ay}}{dt^n}\right) dt \tag{15}$$

$$P_{dyn\,rot} = \frac{\rho}{\delta}B_M\omega^{n+1}\sin\left(n\frac{\pi}{2}\right) \tag{16}$$

$$P_{rot} = \frac{1}{T_{stat}\delta}\int_0^{T_{stat}} \left(\frac{dB_{ax}}{dt}\cdot H_{surfx\,DC} + \frac{dB_{ay}}{dt}\cdot H_{surfy\,DC}\right) dt + \frac{\rho}{\delta}B_M\omega^{n+1}\sin\left(n\frac{\pi}{2}\right) \tag{17}$$

In this context, it is worth noticing that $P_{dyn\,rot}$ is twice larger than $P_{dyn\,alt}$.

III – Comparisons simulations/measurements

Most studies on magnetic losses are limited to alternating conditions in the conventional frequency range (50/60 Hz). This prevalence can be attributed to its practical significance in various applications. The objective is to understand and mitigate losses associated with magnetic field waveforms commonly observed in everyday devices and power systems. Conversely, limited scientific literature on rotational power loss is available, especially in the high field and frequency ranges. This observation can be explained by the relatively specific scenarios where such magnetic field waveforms can be found (high-speed rotating machinery, etc.). Moreover, the absence of industrial equipment for characterization and international standards introduces additional challenges and complexities hindering extensive research efforts.

Still, in the last decade, significant progress in the characterization under rotational magnetization in the high-frequency range can be noticed. Many factors collectively drive the exploration of SFMs in such conditions, including technological advancements, increased computational capabilities, and industry interest, to name but a few [29].

Collecting experimental data from the same articles under alternating and rotational conditions was essential to ensure fair comparisons. This condition ensured that the tested specimens had similar compositions and origins.

Fig. 2 below depicts this paper's first comparison simulations/measurements series. Experimental data were extracted from [33]. Iron-cobalt-vanadium $Fe_{49}Co_{49}V_2$ (FeCo), known as permendur, is tested first for up to 5 kHz in rotational and alternating conditions.

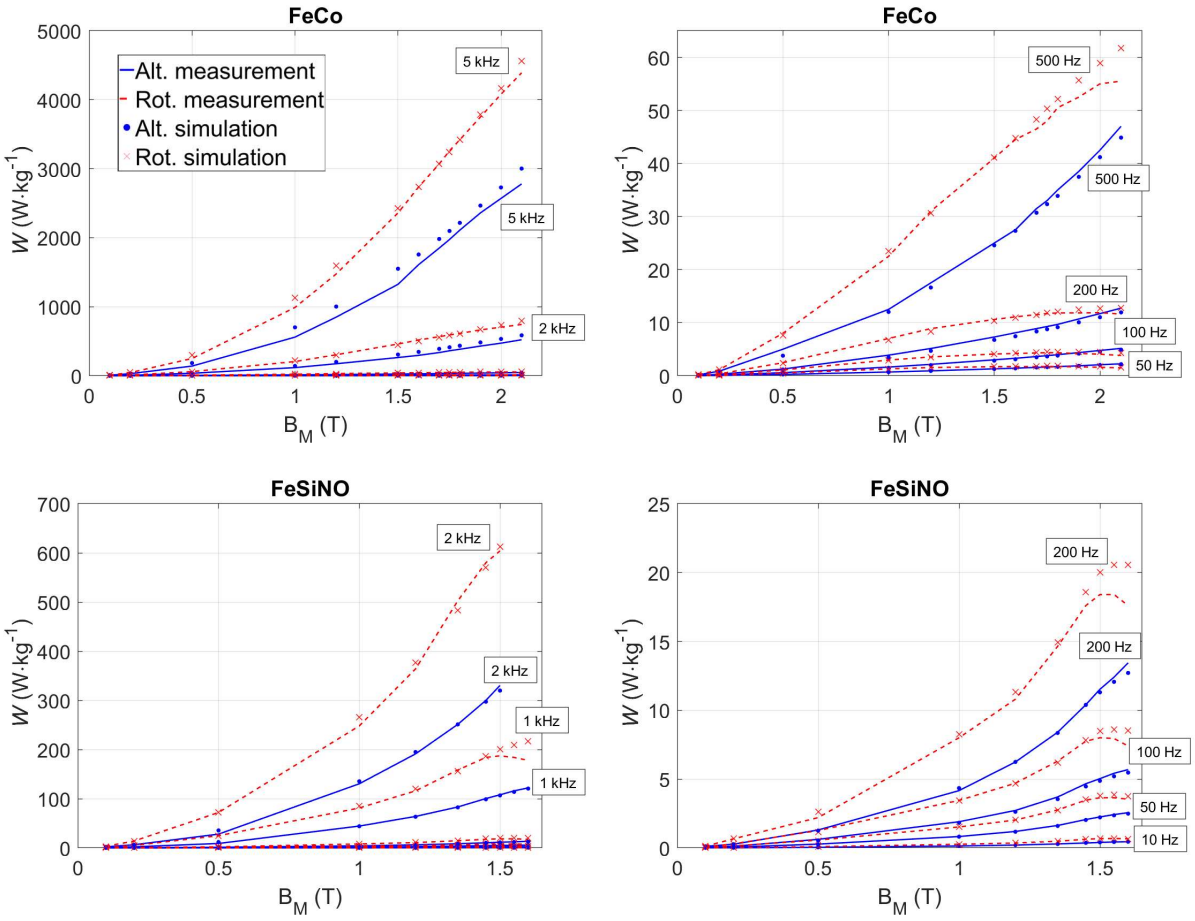

Fig. 2 – Comparisons simulation/measurement[31] under alternating and rotational magnetization for FeCo (top) and NOFeSi (bottom) materials.

The quasi-static contribution P_{stat} under alternating and rotational conditions is not simulated but calculated from the f = 5 Hz experimental measurements. Then, an optimization process based on the relative Euclidean distance (RED(%) [34], Eq. 18) is run to determine the best couple of parameters n and ρ (Table 1).

$$\mathrm{RED}(\%) = \frac{100}{q} \cdot \sum_{i=1}^{q} \frac{\sqrt{\left(P_{meas_i}\left(B_{M_i}\right) - P_{sim_i}\left(B_{M_i}\right)\right)^2}}{\sqrt{\left(P_{meas_i}\left(B_{M_i}\right)\right)^2}} \tag{18}$$

Fig. 2 bottom part shows similar comparisons but for nonoriented electrical steel specimens (NOFeSi). Readers are referred to [33] for more details about the specimens and experimental conditions.

The next series of comparisons concerns oriented grain electrical steel specimens (GOFeSi) and is shown in Fig. 3. The experimental results were gathered from [35]. GOFeSi is deliberately processed to have a preferred crystallographic orientation (GOSS texture, [1][36]), which

enhances its magnetic properties in specific directions. This anisotropic nature complicates the characterization process, especially at high frequencies, where the response can vary significantly depending on the direction of the magnetic field. Still, in [35], authors succeeded in testing GOFeSi for up to f = 2 kHz. In [35], measurements under alternating conditions are acquired in both the rolling direction (RD) and transverse direction (TD). However, this study confines the testing to TD, aligning with the magnetization direction pertinent to electromagnetic applications.

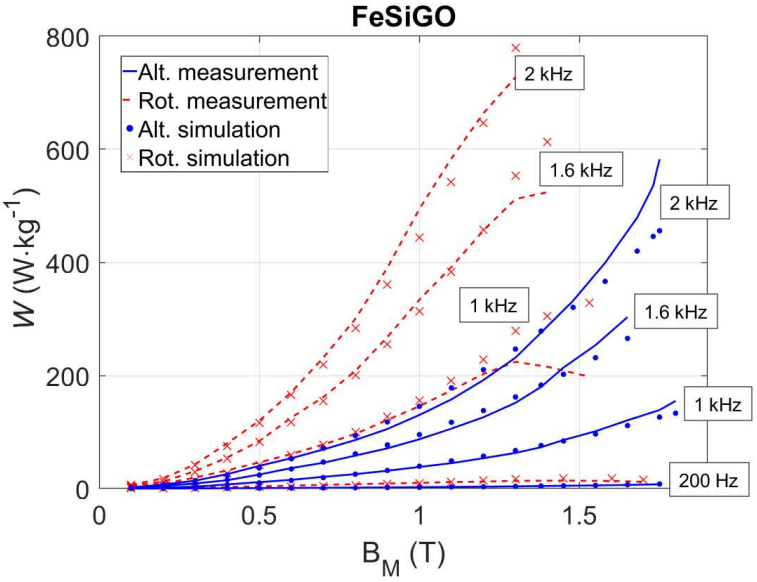

Fig. 3 – Comparisons simulation/measurement[33] under alternating and rotational magnetization for GOFeSi materials.

Fig. 4 shows a series of comparisons in the case of soft magnetic composite (SMC) materials. SMCs offer advantages over traditional ferromagnetic metallic materials due to their unique structure, typically involving insulated magnetic particles dispersed in a non-magnetic matrix [37]. This composite structure reduces eddy current losses and allows for more design flexibility. The SMC experimental results come from [38]. The material tested is referenced as Samaloy TM 500 (Höganäs AB, Sweden).

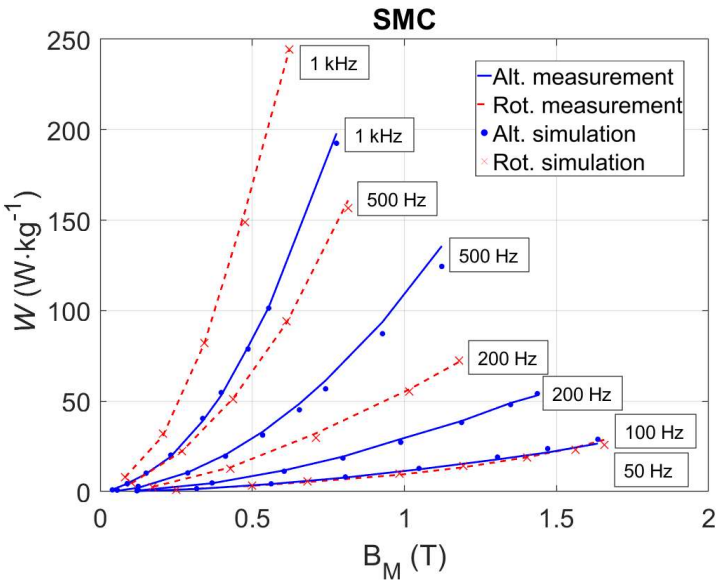

Fig. 4 – Comparisons simulation/measurement[36] under alternating and rotational magnetization for an SMC material (Samaloy TM 500).

The final set of simulation/measurement comparisons (Fig. 5) was conducted using a low-carbon steel material. Unfortunately, we could not find alternating and rotational experimental data extracted from the same article for this material. The rotating results were picked up from [39] and the alternating from [40]. Considering that researchers from the same team wrote both these articles and the material information provided is similar, we believe in the consistency of the tested specimens.

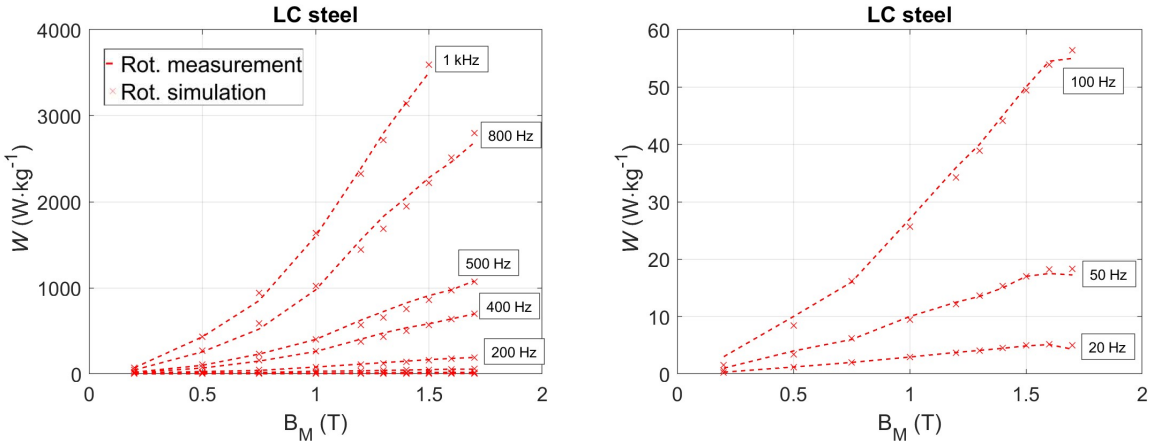

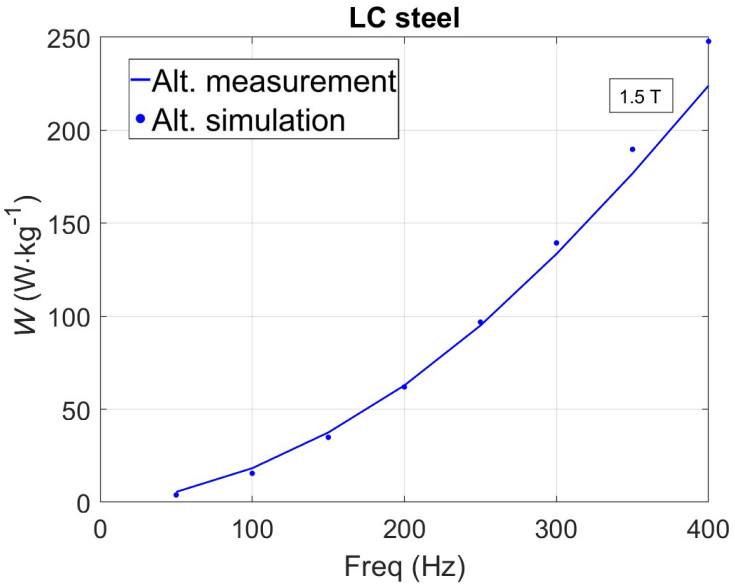

Fig. 5 – Comparisons simulation/measurement[37, 38] under alternating (bottom) and rotational (top) magnetization for low-carbon steel materials.

Table 1 summarizes all experimental and simulation data for all the materials tested. The RED(%) is calculated using both alternating and rotational data.

Table. 1 – Experimental and simulation data for all materials tested

Material	Electrical conductivity σ ($S \cdot m^{-1}$)	Density δ ($kg \cdot m^{-3}$)	Thickness d (m)	ρ ($A \cdot V^{-n} \cdot m^{2n-1}$)	n -	RED (%)
FeCo [31]	$2.27\ 10^{6}$	8120	$0.201\ 10^{-3}$	0.0165	0.934	4.24
NOFeSi [31]	$1.92\ 10^{6}$	7650	$0.194\ 10^{-3}$	0.0536	0.835	3.7
GOFeSi [33]	$2.12\ 10^{6}$	7650	$0.27\ 10^{-3}$	0.024	0.938	9.18
SMC [36]	$1.43\ 10^{4}$	7370	$22\ 10^{-3}$	0.973	0.95	4.59
LC steel [37, 38]	$1.99\ 10^{6}$	7850	$0.64\ 10^{-3}$	0.27	1	6.6

IV – Discussion

Table 1 provides relevant data on a large-scale consideration of the magnetic loss in SFMs. The RED(%) is lower than 5% for most tested materials and always lower than 10%. The relatively high RED(%) of the GOFeSi can be attributed to its strongly anisotropic behavior. This anisotropy could be a source of inhomogeneity between the alternating and rotational observations, increasing the RED(%). The LC steel also has a high RED(%), probably due to the origin of the experimental data gathered from different articles.

It is worth noting that *n* is always larger than 0.8 for all tested materials, meaning that the dynamical behavior is always close to that of a viscous fluid. This observation also confirms the

significant weight of the dissipative loss in the thermodynamic exchanges. ρ, on the other side, shows much more significant amplitude variations. ρ is always in the [0 – 1] interval, but its FeCo value is almost a hundred times lower than SMC's.

Later, in this study, we attempted to establish a relation between n and ρ and the physical and geometrical properties of the tested specimens. When no significant correlation emerged for n, ρ was shown to be quite highly proportional to σd^2 (where σ is the electrical conductivity and d^2 is the thickness), despite its unit depending on n. Fig. 6 below illustrates this proportionality. Based on a linear curve fitting evaluation, this relation can be expressed as:

$$\rho \propto p_1 \sigma d^2 + p_2 \tag{19}$$

with p_1 = 0.135 and p_2 = 0.05. It is worth highlighting the universality of expression 19, which can be applied accurately to all the materials tested in this study.

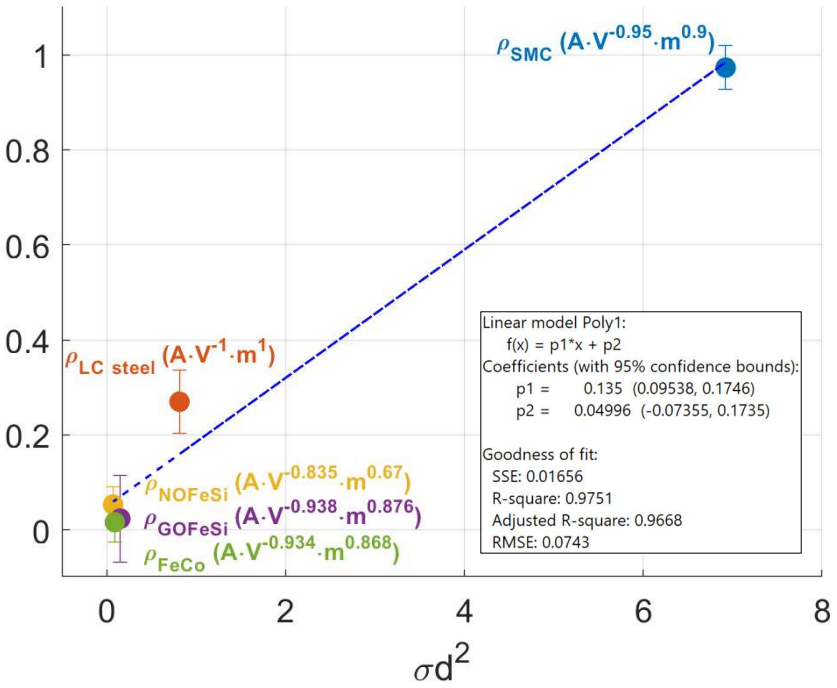

Fig. 6 – ρ vs. σd^2, linear fit and goodness of fit coefficients.

Bertotti and others before him have shown a relationship between σd^2 and the eddy current losses in STL (Eq. 20 [6, 41], where β is a material constant referred to as the magnetic exponent component. β can either be a constant or have functional dependencies, as is the case for SMCs [42]):

$$P_{eddy} = \frac{\pi^2 \sigma d^2 f^2 {B_M}^2}{\beta} \tag{20}$$

Still, this relation was confined to the working conditions of STL. Eq. 19 and the overall results of this study show that a relationship between σd^2 and ρ can be applied more broadly than just STL

working conditions, i.e., under alternating and rotational magnetization for a vast range of materials and on a large frequency bandwidth.

Finally, let us discuss the ratio of two between $P_{dyn\ rot}$ and $P_{dyn\ alt}$. Due to the substantial contrast in the reorganization of magnetic domains under alternating and rotating magnetic fields, the excellent accuracy of the simulation results can solely be attributed to a restricted impact of this effect and, conversely, a significant contribution of the eddy currents. Still, these differences in the magnetization process are probably at the origin of the prediction discrepancy.

V – Conclusion

In this paper, we formulated analytical expressions for the dynamic alternative and rotational magnetic power loss contributions. These expressions rely on the time-fractional derivative of the flux density expressed with a trigonometric function as imposed by the characterization standards. The proposed formulations were validated through comparison simulations/ measurements using extensive experimental data gathered from the most advanced setups and picked up from the scientific literature. Data from five different materials were collected under alternating and rotational conditions, spanning up to at least 1 kHz. The relative Euclidean distance remained below 5% for most materials and consistently below 10%. In standard characterization conditions, our analytical expression gives a rotational power loss contribution twice as high as the alternating one.

When the classic Steinmetz equation required at least three parameters to predict the alternating loss contribution, in this work, the knowledge of the material's electrical conductivity simplifies the dynamic magnetic power loss contribution to a single parameter (the fractional order). For a given specimen, this parameter remains constant for both rotational and alternating contributions.

This work can be viewed from various angles. Key perspectives involve extending the validation process to additional materials, contrasting the dynamic properties emphasized in this study with those of low amplitude and high frequency measured using an impedance LCR-meter (such as in inductance spectroscopy [43]), and further investigating the meaning of n, the ratio between the elastic and the viscous behaviors.

References

[1] Heck, C., 2013. *Magnetic materials and their applications*. Elsevier.

[2] Ferreira, J.A., 1989. *Electromagnetic modelling of power electronic converters*. Springer Science & Business Media.

[3] Mahesh, M., Kumar, K.V., Abebe, M., Udayakumar, L. and Mathankumar, M., 2021. A review on enabling technologies for high power density power electronic applications. *Materials Today: Proceedings*, *46*, pp.3888-3892.

[4] Ferreira, J.A., 1989. *Electromagnetic modelling of power electronic converters*. Springer Science & Business Media.

[5] Kolar, J.W., Drofenik, U., Biela, J., Heldwein, M.L., Ertl, H., Friedli, T. and Round, S.D., 2007, April. PWM converter power density barriers. In *2007 Power Conversion Conference-Nagoya* (pp. P-9). IEEE.

[6] Rodriguez-Sotelo, D., Rodriguez-Licea, M.A., Araujo-Vargas, I., Prado-Olivarez, J., Barranco-Gutiérrez, A.I. and Perez-Pinal, F.J., 2022. Power losses models for magnetic cores: A review. *Micromachines*, *13*(3), p.418.

[7] Zhang, J., Tounzi, A., Benabou, A. and Le Menach, Y., 2021. Detection of magnetization loss in a PMSM with Hilbert Huang transform applied to non-invasive search coil voltage. *Mathematics and Computers in Simulation*, *184*, pp.184-195.

[8] Bertotti, G., 1998. *Hysteresis in magnetism: for physicists, materials scientists, and engineers*. Gulf Professional Publishing.

[9] Bertotti, G., 1988. General properties of power losses in soft ferromagnetic materials. *IEEE Transactions on magnetics*, *24*(1), pp.621-630.

[10] Dlala, E., 2009. Comparison of models for estimating magnetic core losses in electrical machines using the finite-element method. *IEEE Transactions on Magnetics*, *45*(2), pp.716-725.

[11] Raulet, M.A., Ducharne, B., Masson, J.P. and Bayada, G., 2004. The magnetic field diffusion equation including dynamic hysteresis: a linear formulation of the problem. *IEEE transactions on magnetics*, *40*(2), pp.872-875.

[12] Meunier, G. ed., 2010. *The finite element method for electromagnetic modeling*. Wiley.

[13] Hilfer, R. ed., 2000. *Applications of fractional calculus in physics*. World scientific.

[14] IEC 60404-1: 2000, *Magnetic materials, Part 1: Classification, 2000.*

[15] IEC 60404-2: 1998+A1: 2008, *Magnetic materials, Part 2: Methods of measurement of the magnetic properties of electrical steel strip and sheet by means of an Epstein frame, 2008.*

[16] IEC 60404-3: 2010, *Magnetic materials, Part 3: Methods of measurement of the magnetic properties of electrical steel strip and sheet by means of a single sheet tester, 2010.*

[17] Kleinz, M. and Osler, T.J., 2000. A child's garden of fractional derivatives. *The college mathematics journal*, *31*(2), pp.82-88.

[18] Silveyra, J.M., Ferrara, E., Huber, D.L. and Monson, T.C., 2018. Soft magnetic materials for a sustainable and electrified world. *Science*, *362*(6413), p.eaao0195.

[19] Katugampola, U.N., 2011. A new approach to generalized fractional derivatives. *arXiv preprint arXiv:1106.0965*.

[20] Podlubny, I., 1998. *Fractional differential equations: an introduction to fractional derivatives, fractional differential equations, to methods of their solution and some of their applications*. Elsevier.

[21] Tenreiro Machado, J.A., Silva, M.F., Barbosa, R.S., Jesus, I.S., Reis, C.M., Marcos, M.G. and Galhano, A.F., 2010. Some applications of fractional calculus in engineering. *Mathematical problems in engineering*, *2010*.

[22] Stein, E.M. and Shakarchi, R., 2010. *Complex analysis* (Vol. 2). Princeton University Press.

[23] Rüdinger, F., 2006. Tuned mass damper with fractional derivative damping. *Engineering Structures*, *28*(13), pp.1774-1779.

[24] Arthi, G., Park, J.H. and Suganya, K., 2019. Controllability of fractional order damped dynamical systems with distributed delays. *Mathematics and Computers in Simulation*, *165*, pp.74-91.

[25] Findley, W.N. and Davis, F.A., 2013. *Creep and relaxation of nonlinear viscoelastic materials*. Courier corporation.

[26] Ducharne, B. and Sebald, G., 2022. Fractional derivatives for the core losses prediction: State of the art and beyond. *Journal of Magnetism and Magnetic Materials*, p.169961.

[27] Ducharne, B. and Sebald, G., 2022. Combining a fractional diffusion equation and a fractional viscosity-based magneto dynamic model to simulate the ferromagnetic hysteresis losses. *AIP Advances*, *12*(3).

[28] B. Ducharne, H. Hamzehbahmani, Y. Gao, P. Fagan, G. Sebald, High-frequency behavior of grain-oriented magnetic steel laminations and spatial distribution of the loss contributions. *Fractal and fractional*, 2023, under review.

[29] Zurek, S., 2017. *Characterisation of soft magnetic materials under rotational magnetisation*. CRC Press.

[30] Tumanski, S., 2016. *Handbook of magnetic measurements*. CRC press.

[31] Ducharne, B., Zurek, S. and Sebald, G., 2022. A universal method based on fractional derivatives for modeling magnetic losses under alternating and rotational magnetization conditions. *Journal of Magnetism and Magnetic Materials*, *550*, p.169071.

[32] Ducharne, B., Zurek, S., Daniel, L. and Sebald, G., 2022. An anisotropic vector hysteresis model of ferromagnetic behavior under alternating and rotational magnetic field. *Journal of Magnetism and Magnetic Materials*, *549*, p.169045.

[33] Appino, C., de La Barrière, O., Beatrice, C., Fiorillo, F. and Ragusa, C., 2014. Rotational magnetic losses in nonoriented Fe–Si and Fe–Co laminations up to the kilohertz range. *IEEE Transactions on Magnetics*, *50*(11), pp.1-4.

[34] Fagan, P., Ducharne, B., Zurek, S., Domenjoud, M., Skarlatos, A., Daniel, L. and Reboud, C., 2022. Iterative methods for waveform control in magnetic measurement systems. *IEEE Transactions on Instrumentation and Measurement*, *71*, pp.1-13.

[35] Yue, S., Li, Y., Yang, Q., Zhang, K. and Zhang, C., 2019. Comprehensive investigation of magnetic properties for Fe–Si steel under alternating and rotational magnetizations up to kilohertz range. *IEEE Transactions on Magnetics*, *55*(7), pp.1-5.

[36] Goss, N.P., COLD METAL PROCESS CO, 1934. *Electrical sheet and method and apparatus for its manufacture and test*. U.S. Patent 1,965,559.

[37] Perigo, E.A., Weidenfeller, B., Kollár, P. and Füzer, J., 2018. Past, present, and future of soft magnetic composites. *Applied Physics Reviews*, *5*(3).

[38] Li, Y., Zhu, J., Yang, Q., Lin, Z.W., Guo, Y. and Zhang, C., 2011. Study on rotational hysteresis and core loss under three-dimensional magnetization. *IEEE Transactions on Magnetics*, *47*(10), pp.3520-3523.

[39] Appino, C., Hamrit, O., Fiorillo, F., Ragusa, C., de La Barrière, O., Mazaleyrat, F. and LoBue, M., 2015. Skin effect in steel sheets under rotating induction. *International Journal of Applied Electromagnetics and Mechanics*, *48*(2-3), pp.247-254.

[40] Fiorillo, F., 2004. *Characterization and measurement of magnetic materials*. Academic Press.

[41] Bertotti, G., 1988. General properties of power losses in soft ferromagnetic materials. *IEEE Transactions on magnetics*, *24*(1), pp.621-630.

[42] Kollár, P., Birčáková, Z., Füzer, J., Bureš, R. and Fáberová, M., 2013. Power loss separation in Fe-based composite materials. *Journal of magnetism and magnetic materials*, *327*, pp.146-150.

[43] Ducharne, B., Zhang, S., Sebald, G., Takeda, S. and Uchimoto, T., 2022. Electrical steel dynamic behavior quantitated by inductance spectroscopy: Toward prediction of magnetic losses. *Journal of Magnetism and Magnetic Materials*, *560*, p.169672.